# Combined use of x-ray fluorescence microscopy, phase contrast imaging for high resolution quantitative iron mapping in inflamed cells

C Gramaccioni[1,4], A Procopio[2], G Farruggia[2], E Malucelli[2], S Iotti[2], A Notargiacomo[3], M Fratini[4,5], Y Yang[6], A Pacureanu[6], P Cloetens[6], S Bohic[6], L Massimi[4], A Cutone[7], P Valenti[7], L Rosa[7], F Berlutti[7] and S Lagomarsino[4]

[1] Department of Physics, University of Cosenza, Arcavata di Rende, (Cosenza), Italy

[2] Department of Pharmacy and biotechnology, University of Bologna, Bologna, Italy

[3] Institute for Photonics and Nanotechnologies - CNR, Roma Italy

[4] CNR-Nanotec, c/o Department of Physics University of Sapienza, Roma, Italy

[5] Fondazione Santa Lucia, Roma, Italy

[6] ESRF, Grenoble, France

[7] Department of Public Health and Infectious Diseases, University of Sapienza, Roma, Italy

**Abstract.** X-ray fluorescence microscopy (XRFM) is a powerful technique to detect and localize elements in cells. To derive information useful for biology and medicine, it is essential not only to localize, but also to map quantitatively the element concentration. Here we applied quantitative XRFM to iron in phagocytic cells. Iron, a primary component of living cells, can become toxic when present in excess. In human fluids, free iron is maintained at $10^{-18}$ M concentration thanks to iron binding proteins as lactoferrin (Lf). The iron homeostasis, involving the physiological ratio of iron between tissues/secretions and blood, is strictly regulated by ferroportin, the sole protein able to export iron from cells to blood. Inflammatory processes induced by lipopolysaccharide (LPS) or bacterial pathoge inhibit ferroportin synthesis in epithelial and phagocytic cells thus hindering iron export, increasing intracellular iron and bacterial multiplication. In this respect, Lf is emerging as an important regulator of both iron and inflammatory homeostasis. Here we studied phagocytic cells inflamed by bacterial LPS and untreated or treated with milk derived bovine Lf. Quantitative mapping of iron concentration and mass fraction at high spatial resolution is obtained combining X-ray fluorescence microscopy, atomic force microscopy and synchrotron phase contrast imaging.

## 1. Introduction

Iron is an essential element for cell growth and proliferation being involved in fundamental processes, such as DNA replication and energy production. However, iron can also be toxic when present in excess because of its capacity to donate electrons to oxygen. Therefore, iron homeostasis is strongly regulated

both at tissue/secretion and cell levels [1]. In human fluids free iron is maintained at low concentration ($10^{-18}$M) thanks to iron binding proteins as lactoferrin (Lf) in secretions and transferrin in blood [1]. In fact, Lf is the most important iron binding glycoprotein of natural immunity [1, 2]. Iron homeostasis is also tightly related to inflammation and infection [1, 3]. In particular, macrophages are specialized cells involved in these processes regulating iron influx in human fluids [4]. In inflammation and infection induced by lipopolysaccharide (LPS) or bacterial pathogens, the synthesis of ferroportin, the sole protein able to export iron from macrophages to blood, is inhibited thus hindering iron export, increasing intracellular iron, bacterial multiplication and inflammatory processes. Recently, Lf has been found to be an important regulator of iron homeostasis and a potent anti-inflammatory factor [1,5]. Conversely, very little (if anything) is known about the effect of Lf on the concentration and distribution of iron in inflamed and non-inflamed macrophages. The present work has two main aims: i) to demonstrate the possibility to quantitatively map the intracellular iron mass fraction and concentration at nanoscale spatial resolution in macrophages using combination of several techniques, i.e. X-ray Fluorescence Microscopy (XRFM), Atomic Force Microscopy (AFM) and Phase Contrast Imaging (PCI); ii) to compare the iron maps of the cells inflamed by bacterial LPS and untreated or treated with milk derived bovine Lf (bLf). In previous works [6, 7], we utilized X-ray absorption microscopy instead of PCI. However, in this case the relatively high energy photons (17 keV) would give no contrast in absorption mode, and phase contrast mode, which is sensitive to tiny variations of refraction index, has been used to obtain visible contrast.

## 2. Experimental methods

### 2.1 Sample preparation
J774.2 macrophages (Sigma Aldrich) were cultured in RPMI 1640 medium supplemented with 20% heat-inactivated foetal calf serum (FCS), 100 unit/ml of penicillin and 100 µg/ml of streptomycin on 1×1 mm², 200-nm-thick silicon nitride ($Si_3N_4$) membrane windows, mounted on a 5×5 mm² Si frame (purchased from www.Silson.co.uk) previously sterilized in ethanol. Cells were inflamed using *E. coli* LPS (1µg/ml) (InvivoGen). The inflamed cells were untreated or treated with bLf (100µg/ml) (Morinaga Milk Industries, Japan). After 48h, cells were rinsed with 100 mM ammonium acetate, cryofixed by plunge freezing in liquid ethane bath cooled with liquid nitrogen and then dehydrated in vacuum at low temperature overnight.

### 2.2 XRFM, PCI and AFM measurements
Dehydrated cells mounted on the $Si_3N_4$ membrane windows were carefully examined with optical microscope and selected with the following criteria: integrity, dimensions and distance from other cells. AFM measurements were performed on selected cells before XRFM and PCI measurements. AFM topography maps were collected off-line by using a Digital Instruments D3100 microscope equipped with a Nanoscope IIIa controller. The AFM was operated in ambient air using the tapping mode at a resonance frequency of about 260 kHz. Commercial monolithic silicon tips were employed, with an apex curvature radius in the 5-10 nm range and a nominal force constant of 40 $Nm^{-1}$. AFM maps with size of the order of 50 µm were collected with lateral spatial resolution of ~100 nm and accuracy in the cell thickness measurement of about 30 nm. Images were collected without any real-time filtering or flattening, and were post-processed to eliminate all the possible artefacts [6]. The Fig. 1 shows the AFM topographic data of a cell treated with LPS in the absence of bovine Lf (bLf).
The X-ray measurements were carried out at the beamline ID16A-NI at the European synchrotron radiation facility (ESRF, Grenoble, France) with spatial resolution of 100 nm (dwell time 50 ms) for XRFM and 50 nm for PCI. In this work, the energy was set to 17 keV for all experiments. The samples were positioned in the focal plane of the KB system, translated by piezo-stages in the directions perpendicular to the beam. The X-ray fluorescence emission lines of several elements were collected by the silicon drift energy dispersive detectors positioned in the horizontal plane at 95° of the incoming X-ray beam. After acquisition the fluorescence spectra were analysed using the PyMCA free program [8], and the total counts of the Fe K lines, after subtraction of the backgrounds, were mapped as a function

of the sample position with respect to the incoming beam. The resulting fluorescence map for the same cell of Figure 1 is displayed in Fig. 2.

The PC projections were acquired at four different distances (29 mm, 30 mm, 34 mm, 44 mm) downstream of the X-ray focus resulting in magnified Fresnel patterns collected by a highly sensitive charge-coupled device (CCD) camera. For each 4 distances, we have acquired 17 images, 10 references, with 0.25 s, and 20 dark-fields. A complex procedure to retrieve the phase has been carried out [9, 10]. The result for the same cell is shown in Fig. 3.
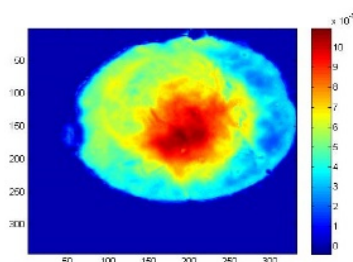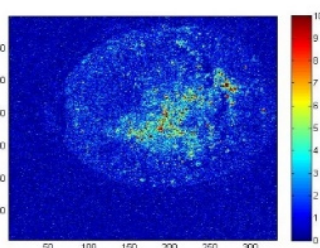


**Figure 1.** AFM topographic map of LPS-treated cell [μm]



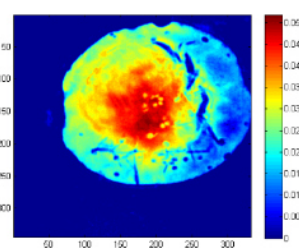**Figure 2.** Fluorescence intensity iron map of LPS-treated cell



**Figure 3.** 2D Phase Reconstruction map of LPS-treated cell

### 3. Results and conclusion

The experimental results presented in Figs 1, 2 and 3, allowed to calculate both the iron mass fraction and the concentration. The mass fraction (Fig. 4) is obtained normalizing the fluorescence map with the projected electron density derived by the analysis of the PCI. The concentration (Fig. 5) is instead obtained by normalizing the fluorescence map with the volume of each pixel, as derived by the AFM. Both Figs 4 and 5 refer to a cell treated with LPS in the absence of bLf.
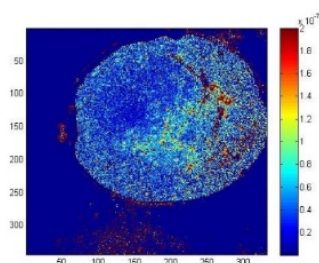


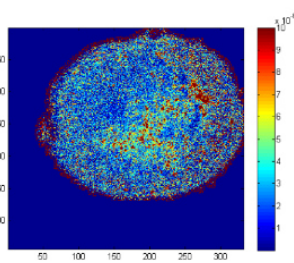**Figure 4.** Iron mass fraction map of LPS-treated cell in the absence of bLf



**Figure 5.** Iron concentration map of LPS-treated cell in the absence of bLf
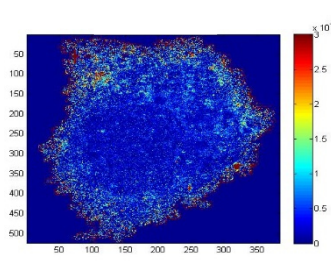


**Figure 6.** Iron concentration map of LPS-treated cell in the presence of bLf

It is noteworthy that the distribution maps of the iron mass fraction and of the iron concentration in LPS-treated cell without Lf are very similar (Figures 4 and 5), confirming the validity of the experimental approach. In Fig. 6 the iron concentration map of LPS-treated cell in the presence of Lf is shown. Preliminary quantitative evaluation indicated that intracellular iron concentrations in LPS-inflamed cells untreated or treated with bLf were quite different (35 and 7 nM, respectively) in agreement with previously reported data on ferroportin synthesis [1, 4, 5]. Interestingly, the cellular iron distribution in LPS-treated cell (Fig.5) appeared different respect to that of LPS-treated cell in the presence of bLf (Fig.6) being located around the cytoplasm membrane cell, suggesting the reduction of its export probably associated to the inhibition of ferroportin [4, 5].

In conclusion, for the first time we have shown that with proper combination of different techniques, it is possible to obtain quantitative information at nanoscale spatial resolution about iron concentration and distribution in inflamed cells, opening the way to more complex studies on the role and therapeutic efficacy of Lf in restoring iron and inflammatory homeostasis disorders. This study has been conducted on freeze dried cells, but we have also analyzed frozen hydrated cells, the closest ones to the living cells, using nanotomography instead of AFM to measure the volume of the cells. The analysis here reported has great potentiality to improve the comprehension of the mechanisms of iron homeostasis in conditions close to the living one.

## References

[1] Paesano R, Natalizi T, Berlutti Fand Valenti P 2012 Body iron delocalization: the serious drawback in iron disorders in both developing and developed countries Pathog. Glob. Health 106 200-16

[2] Valenti P and Antonini G 2005 Lactoferrin: an important host defence against microbial and viral attack *Cell Mol Life Sci.* **62**(22) 2576-87.

[3] Valenti P and al. 2015 Lactoferrin and cystic fibrosis airway infection *Diet and Exercise in Cystic Fibrosis* **30** 259

[4] Cairo G, Recalcati S, Mantovani A andLocati M 2011 Iron trafficking and metabolism in macrophages: contribution to the polarized phenotype *Trends Immunol* **32** 241–47

[5] Cutone A, Frioni A, Berlutti F, Valenti P, Musci G and Bonaccorsi di Patti MC 2014 Lactoferrin prevents LPS-induced decrease of the iron exporter ferroportin in human monocytes/macrophages. *Biometals* **27** 807-13

[6] Lagomarsino S, Iotti S, Farruggia G, Cedola A, Trapani V, Fratini M and al. 2011 Intracellular concentration map of magnesium in whole cells by combined use of X-ray fluorescence microscopy and atomic force microscopy *Spectrochim Acta Part B At Spectrosc.* **66** (11–12) 834–40

[7] Malucelli E, Iotti S, Gianoncelli A, Fratini M, Merolle L, Notargiacomo A and al. 2014 Quantitative Chemical Imaging of the Intracellular Spatial Distribution of Fundamental Elements and Light Metals in Single Cells *Anal. Chem.* **86** (10) 5108–15

[8] Sole V, Papillon E, Cotte M, Walter P and Susini J 2007 A multiplatform code for the analysis of energy dispersive X-ray fluorescence spectra *Spectrochim. ActaPart B At. Spectrosc.* **62** 63–8

[9] Cloetens P, Ludwig W, Baruchel J, Dyck, J V, Landuyt J V and al. 1999 Holotomography: quantitative phase tomography with micrometer resolution using hard synchrotron radiation X-rays *Appl. Phys. Lett.* **75** 2912–14

[10] Langer M, Cloetens P, Guigay JP and Peyrin F 2008 Quantitative comparison of direct phase retrieval algorithms in in-line phase tomography Med. *Phys.* **35** (10) 4556–66

[11] E. Kosior , Bohic S, Suhonen H, Ortega R, Devès G, Carmona A and al. 2012 Combined use of hard X-ray phase contrast imaging and X-ray fluorescence microscopy for sub-cellular metal quantification *J Struct Biol.* **177** (2) 239–47

[12] Malucelli E, Fratini M, Notargiacomo A, Gianoncelli A, Merolle L and al. 2016 Where is it and how much? Mapping and quantifying elements in single cells *Analyst.* **141** 5221-35